Available online at www.sciencedirect.com
ScienceDirect
Applied Surface Science 253 (2007) 9124–9129
applied surface science
www.elsevier.com/locate/apsusc

Correlation between substrate bias, growth process and structural properties of phosphorus incorporated tetrahedral amorphous carbon films

Aiping Liu *, Jiaqi Zhu *, Jiecai Han, Huaping Wu, Zechun Jia

Center for Composite Materials, Harbin Institute of Technology, P.O. Box 3010, Yikuang Street 2, Harbin 150080, PR China

Received 10 February 2007; received in revised form 17 May 2007; accepted 17 May 2007
Available online 24 May 2007

Abstract

We investigate the growth process and structural properties of phosphorus incorporated tetrahedral amorphous carbon (ta-C:P) films which are deposited at different substrate biases by filtered cathodic vacuum arc technique with PH_3 as the dopant source. The films are characterized by X-ray photoelectron spectroscopy (XPS), atomic force microscopy, Raman spectroscopy, residual stress measurement, UV/VIS/NIR absorption spectroscopy and temperature-dependent conductivity measurement. The atomic fraction of phosphorus in the films as a function of substrate bias is obtained by XPS analysis. The optimum bias for phosphorus incorporation is about −80 V. Raman spectra show that the amorphous structures of all samples with atomic-scaled smooth surface are not remarkably changed when PH_3 is implanted, but some small graphitic crystallites are formed. Moreover, phosphorus impurities and higher-energetic impinging ions are favorable for the clustering of sp^2 sites dispersed in sp^3 skeleton and increase the level of structural ordering for ta-C:P films, which further releases the compressive stress and enhances the conductivity of the films. Our analysis establishes an interrelationship between microstructure, stress state, electrical properties, and substrate bias, which helps to understand the deposition mechanism of ta-C:P films.

PACS : 81.15.Ef; 78.30.Ly; 78.66.Jg; 68.37; 62.40.+i

Keywords: Phosphorus incorporated tetrahedral amorphous carbon; Filtered cathodic vacuum arc; Substrate bias; Microstructure; Residual stress; Optical gap

1. Introduction

Tetrahedral amorphous carbon (ta-C) films have been applied in many electronic devices because of their attractive chemical inertness, excellent optical and mechanical properties. In previous reports, boron has been used as an electrically active p-type dopant in carbon films [1]. As an n-type impurity nitrogen has been widely studied because of its size similar to carbon [2]. Phosphorus is another potential element to develop n-type doped ta-C films, and believed more active than nitrogen in nature. Currently, different techniques such as filtered cathodic vacuum arc (FCVA), ion-beam sputtering, pulsed laser, plasma immersion ion implantation and chemical vapor deposition [3–7], and various dopant sources including red phosphorus, trimethylphosphite ($P(OCH_3)_3$) and phosphine (PH_3) [3–9] have been used to prepare phosphorus incorporated a-C (a-C:P) films. These films exhibit many outstanding properties which make them appropriate for the application as photovoltaic solar cells [4,7], semiconductor field emitters [8] or biomedical coatings [6]. However, most effort has been devoted to the investigation about the structural and electrical characteristics of a-C:P films [3,5,7]. To our knowledge, there are few reports on the growth process or stress states of a-C:P films [9].

In the present paper, phosphorus incorporated ta-C (ta-C:P) films are prepared by FCVA technology. PH_3 is adopted to introduce phosphorus into the carbon network as an intentional impurity. Considering previous work [9], we provide a special report on ta-C:P films deposited at the substrate bias varying from −20 to −2000 V. A systemic Raman analysis ranging from 600 to 3500 cm^{-1} is carried out to evaluate the structural rearrangement of ta-C films after phosphorus implantation. The changes in intrinsic stress and electrical behavior induced by phosphorus impurities are further discussed in the following.

* Corresponding authors. Tel.: +86 451 86417970; fax: +86 451 86417970.
E-mail addresses: liuaiping1979@gmail.com (A. Liu), zhujq@hit.edu.cn (J. Zhu).

0169-4332/$ – see front matter © 2007 Elsevier B.V. All rights reserved.
doi:10.1016/j.apsusc.2007.05.040

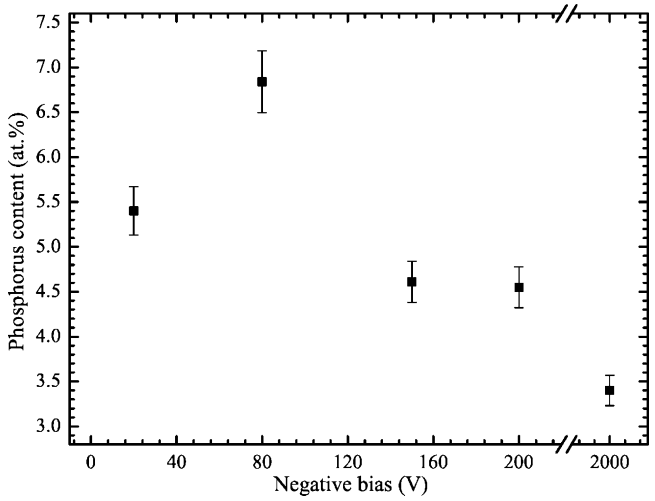

Fig. 1. Relationship between phosphorus content in ta-C:P films and negative substrate bias.

2. Experimental details

Ta-C and ta-C:P films with thickness of ~80 nm were synthesized on p-type silicon wafers, quartz or insulating glass substrates by FCVA system [10]. The graphite cathode (purity 99.999%) was used as the carbon source. Prior to deposition, the vacuum chamber was pumped down to 2×10^{-6} Torr and the pulse substrate bias was −20, −80, −150, −200 and −2000 V, respectively. The arc current was set to 60 A, and the magnetic field intensity of the filtered duct with an inner diameter of 160 mm was 40 mT. When 10-sccm PH_3 (purity 99.9999%) gas was introduced into the same vacuum chamber and arrived at the dynamical balance, the arc was ignited by contacting the graphite anode against the graphite cathode, and then the mixed plasma of carbon and PH_x (x = 0–2) (formed due to ion collisions) passed through a double bend off-plane filter and was deposited on the substrates.

X-ray photoelectron spectroscopy (XPS) analysis was made using a PHI ESCA 5700 spectrometer with Al K_α line (1486.6 eV) as the X-ray source. The compositions of the films were quantified for phosphorus and carbon elements from the total areas of XPS signals (P 2p and C 1s core level spectra were located at 132.4 ± 0.2 and 285.4 ± 0.2 eV, respectively). When the sensitivity factor of C was taken to be 1.00, the sensitivity factor of P equaled to 1.61. The surface morphology of all samples was observed via a Digital Instruments Dimension 3100 atomic force spectroscope (AFM), and the root mean square (RMS) surface roughness was calculated at five different areas ($1 \times 1\ \mu m^2$). Raman analysis over the range from 600 to 3500 cm^{-1} was performed at room temperature on a Jobin Yvon Labram HR 800 spectrometer with 458-nm Ar^+ laser as the excitation source. Laser power was 20 mW, and typical data acquisition time was 100 s. The stress, σ_R, in the films was determined from the curvature measurements of silicon wafer before and after films deposition using a Dektak III profilometer and well-known Stoney's equation [11]:

$$\sigma_R = \frac{E_S}{6(1-\upsilon_S)} \frac{t_S^2}{t_f} \left(\frac{1}{R_2} - \frac{1}{R_1} \right)$$

where E_S is Young's modulus of the substrate; υ_S is Poisson's ratio of the substrate; $E_S/(1-\upsilon_S)$ is biaxial modulus of the substrate and equals to 180.5 GPa; t_S and t_f are the thickness of the substrate and the films; R_1 and R_2 are the radii of curvature

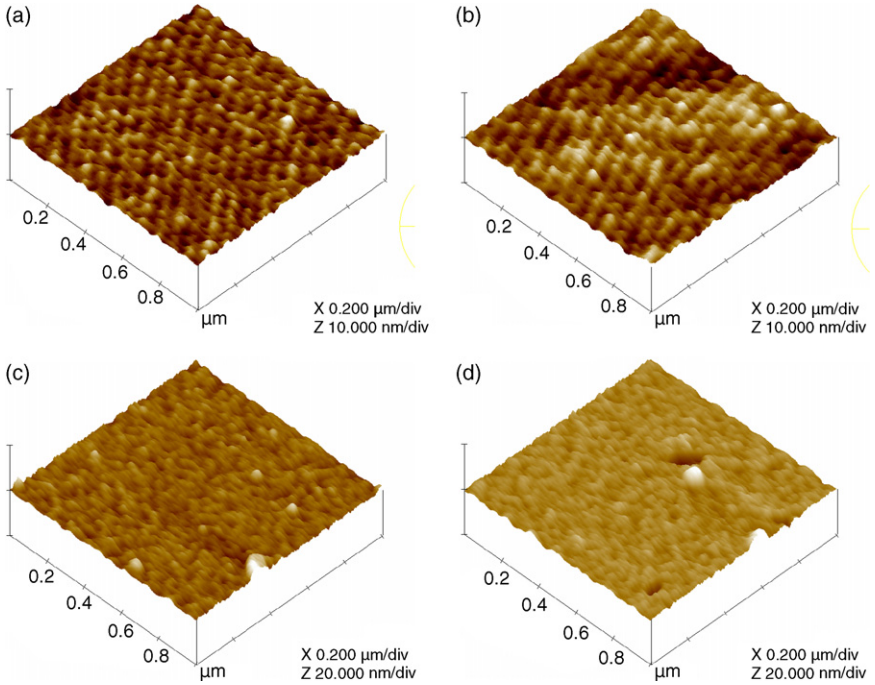

Fig. 2. AFM images of ta-C and ta-C:P films deposited at different biases: (a) ta-C at −80 V; (b) ta-C:P at −20 V; (c) ta-C:P at −80 V; (d) ta-C:P at −2000 V. The dimension in the z-direction is 10 nm div^{-1} in (a) and (b), and 20 nm div^{-1} in (c) and (d).

for the substrate before and after films deposition, respectively. UV/VIS/NIR absorption spectra of ta-C:P films deposited on quartz substrates were carried out by a PerkinElmer Lambda 950 spectrometer ranging from 200 to 1500 nm with a spectral resolution of 1 nm. The optical gap was estimated by using E_{04} that was defined as the energy at which the optical absorption coefficient assumed 10^4 cm^{-1} [12]. The resistance of all samples grown on glass substrates was measured over the temperature range of 293–573 K via electrometer (Keithley 617) or four-point probe. The activation energy (E_{act}) was extracted from the temperature-dependent conductivity curves on a logarithmic scale.

3. Results and discussion

3.1. Phosphorus content

Fig. 1 shows atomic percentage content of phosphorus over the sum of phosphorus and carbon atoms (P/(C + P)) in ta-C:P films as a function of negative substrate bias. The absolute uncertainty is less than ±0.4 at.%. We can see that the maximum of phosphorus content is obtained at −80 V, while phosphorus fraction decreases when the bias is lower or higher than −80 V. This indicates that −80 V bias is favorable for the incorporation of phosphorus. A similar tendency was observed by Pearce who obtained a maximum value of phosphorus impurities at about −130 V. Pearce explained this due to the collision action of the higher-energetic plasma which significantly dropped the level of phosphorus impurities by sputtering the weakly bonded PH_x species from the surface compared with the more strongly bonded CH_x (x = 0–3) species [9]. Additionally, a slight shift of C 1s spectra from 285.5 to 285.4 eV after phosphorus implantation hints that phosphorus incorporation may increase the sp^2 bonds in graphite with the reduction in diamond-like sp^3 bonds.

3.2. Surface morphology

Fig. 2 illustrates the three-dimensional AFM images of ta-C and ta-C:P films, and all ta-C:P films exhibit smooth and flat surfaces similar to ta-C film. In earlier studies [10], we found that ta-C film which was grown at −80 V bias possessed glassy morphology with the RMS surface roughness around 0.23 nm. The value of the surface roughness further changed between 0.22 and 0.32 nm when different biases were applied. It is worth noticing that the RMS surface roughness of ta-C:P films gradually increases from 0.32 to 0.46 nm with the varying bias from −20 to −2000 V, which indicates that some isolated and irregular tops are dispersed on the film surfaces. We ascribe these changes to the enlarged nanoclusters induced by phosphorus impurities. Therefore, phosphorus impurities play a main role in the development of surface morphology.

3.3. Raman spectra

Raman spectra of ta-C:P films shown in Fig. 3(a) indicate that the lineshapes of all spectra are similar and demonstrate the amorphous structures of the films. We observe three prominent features, i.e. the first-order peak of carbon between 1000 and 1800 cm^{-1}, the second-order peak of carbon between 2400 and 3400 cm^{-1} and the second-order peak of silicon centered at about 980 ± 2 cm^{-1}. No phosphorus-related Raman features are discovered in the low-frequency region as those forecasted by Fuge and Claeyssens [5,13]. This could be due to the existence of another vibration mode correlated to phosphorus, and the frequency of the vibration mode might be undistinguishable from that of first-order carbon vibration [14]. For the purpose of simplicity, we fit the asymmetric first-order and second-order bands with two and three Gaussian lines. The first-order band depends on D peak centered at about 1370 ± 5 cm^{-1} and G peak centered at 1557 ± 10 cm^{-1}. Generally called G peak is attributed to the bond stretching of all pairs of sp^2 atoms in rings as well as chains, while D peak is related to the breathing modes of sp^2 sites only in rings. Further the second-order band is ascribed to three peaks (labeled as D′, G′ and (D + G)′) [15] centered at the approximate frequency positions for 2*ωD (the frequency of D peak), 2*ωG (the frequency of G peak), and the combination of ωD and ωG [16], respectively. Because the second-order band can be clearly seen

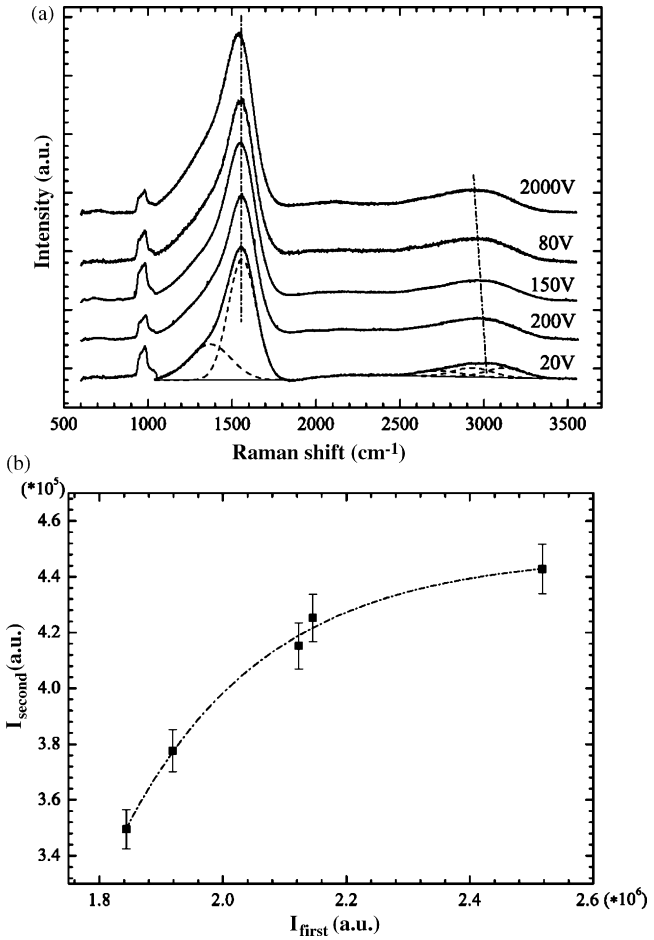

Fig. 3. (a) Raman spectra of ta-C:P films deposited at different biases. Solid lines and dash lines are measured and fitted peaks, respectively; (b) Relationship between integrated intensity of second-order band, I_{second}, and integrated intensity of first-order band, I_{first}, for ta-C:P films prepared at various biases.

when ta-C:P films are annealed at 700 °C with the hydrogen emission from the films [17], we consider that the contribution of CH bonds is negligible for the analysis of Raman spectra. The relationship between the integrated intensity of the second-order band, I_{second}, and the integrated intensity of the first-order band, I_{first}, for ta-C:P films prepared at various substrate biases is shown in Fig. 3(b), and this is consistent with the result of Messina [15].

All fitting parameters including the full width at half maximum (FWHM), peak position and intensity ratio of peaks as a function of substrate bias are plotted in Fig. 4. It can be seen that when substrate bias varies from −20 to −200 V, G peak firstly shifts down to lower frequency and subsequently moves up to higher frequency; a minimum in G-peak FWHM and a maximum in D-peak FWHM are simultaneously obtained at −80 V bias. Correspondingly, intensity ratio of D peak and G peak, $I_{(D)}/I_{(G)}$, arrives at its maximum at the same condition. Similar trends are also obtained from the fitting parameters of D′ and G′ peaks. However, when a higher −2000 V bias is applied, all values become sharper than those obtained at −80 V bias. According to the viewpoint of Ferrari, $I_{(D)}/I_{(G)}$ ratio is a crucial parameter to quantify the sp^3 or sp^2 content [18]. The increase in $I_{(D)}/I_{(G)}$ ratio from 0.30 to 0.44 indicates a clustering of sp^2 sites, especially, an evolution of sp^2 configurations from olefinic groups to rings. This result is practically identical to the downshift of G peak because aromatic bonds are longer than olefinic bonds in chains and hold lower vibration frequencies [18]. Therefore, we can infer from the above analysis that under the lower bias (from −20 to −200 V), phosphorus impurities promote the clustering of the isolated sp^2 sites distributed in the sp^3 skeleton and develop them into larger sizes. This result is in good agreement with those reported in [13] and [19]. However, at the higher −2000 V bias, high impinging energy releases the sp^2 sites to form higher-ordering ring structures [20]. The conclusion can be confirmed from the variation of second-order Raman bands of carbon, which suggests the existence of small graphitic crystallites due to a finite crystal-size effect [21,22].

3.4. Intrinsic stress

Fig. 5 demonstrates a monotonic decrease of the compressive stress with increasing substrate bias. No severe relationship between sp^3 or sp^2 fraction and the compressive stress is observed [23]. The contribution of phosphorus impurities and impinging energy to the relief of the compressive stress for ta-C:P films can be explained as the local distribution of atoms [24]. When phosphorus atoms are introduced into the carbon network, the carbon atoms near to phosphorus atoms may be induced to transform sp^2-hybridized sites. Further higher-energetic particles release excess energy to lead local metastable sp^3 sites to form thermodynamically stable sp^2

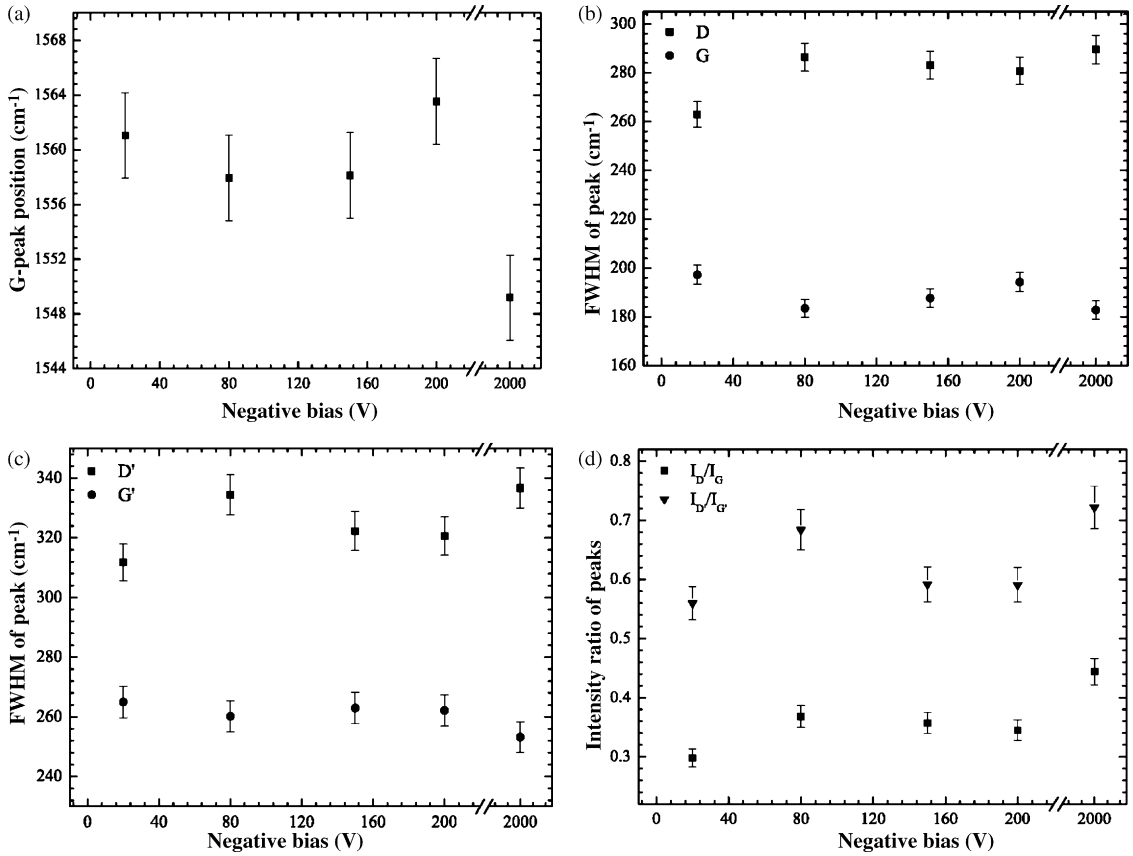

Fig. 4. Fitting parameters of Raman spectra as a function of substrate bias: (a) G-peak position; (b) FWHMs of D peak and G peak, (c) FWHMs of D′ peak and G′ peak; (d) $I_{(D)}/I_{(G)}$ and $I_{(D')}/I_{(G')}$ ratios.

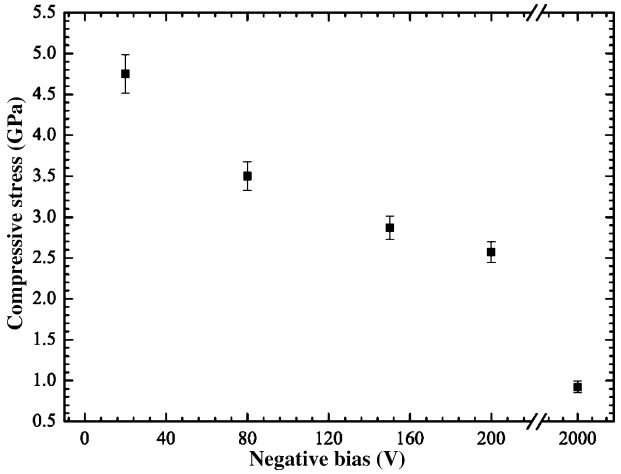

Fig. 5. Dependence of intrinsic compressive stress and substrate bias for ta-C:P films.

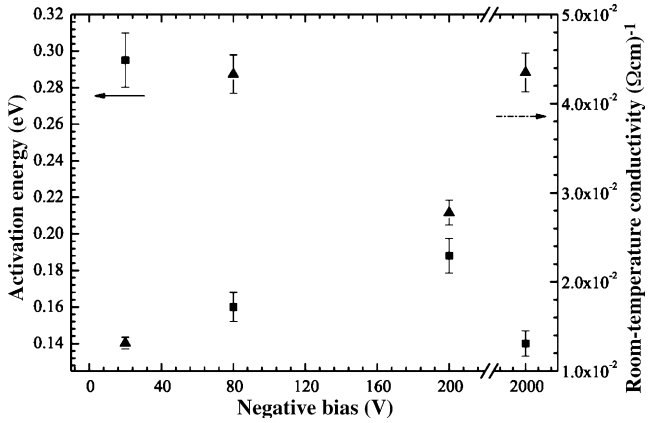

Fig. 7. Room-temperature conductivity and activation energy as a function of substrate bias.

sites. Since sp^2 sites are smaller than sp^3 sites in the in-plane size, the formation of sp^2 sites with their π planes aligned in the plane of compression will relieve the biaxial compressive stress [25].

3.5. Optical and electrical behaviors

The relationship between the optical gap, E_{04}, and the substrate bias is displayed in Fig. 6. It is generally believed that the optical gap in amorphous carbon films is determined as the gap between the π and π^* states on sp^2 sites [26]. Due to phosphorus impurities and higher-energetic particles increase sp^2 sites and the densities of the π and π^* states, the smaller E_{04} values are obtained at -80 and -2000 V bias. However, whether the phosphorus atoms contribute to the effective n-type doping or alloy with the carbon network is still unclear. To deal with the problem, some conductivity measurements are carried out to analyze the form of phosphorus impurities in the carbon network. Fig. 7 shows the changes of room-temperature conductivity and activation energy with substrate bias. The conductivity increases from 1.3×10^{-2} to 4.4×10^{-2} $(\Omega cm)^{-1}$ and activation energy decreases from 0.30 to 0.14 eV when the substrate bias varies from -20 to -2000 V. The Fermi level (E_F) is calculated from the band gap and activation energy using the midgap as the reference energy level. It seems that E_F moves up towards the conduction band edge [3], accompanying by several orders of magnitude increase in room-temperature conductivity (the conductivity of ta-C film is about 10^{-8}–10^{-7} $(\Omega cm)^{-1}$) when the substrate bias increases from -20 to -2000 V. So phosphorus atoms may replace partial carbon atoms by the substitutional doping [7] and provide their electrons as ionized donors to hopping conduction [3,7,8]. This is responsible for the remarkable enhancement of the film conductivity.

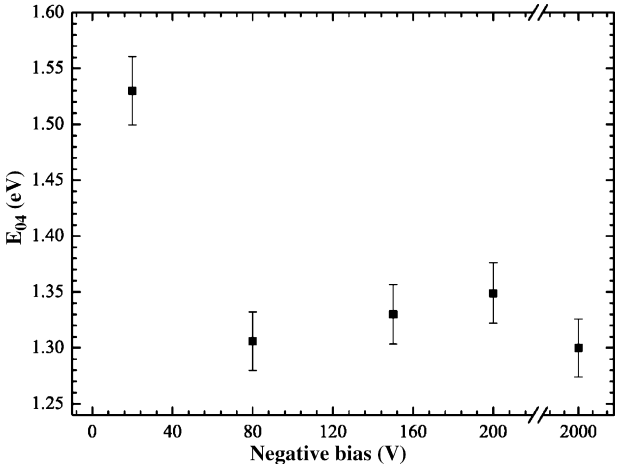

Fig. 6. Optical gap vs. negative substrate bias applied during deposition.

3.6. Deposition mechanism

Based on the above analysis, we suggest that the deposition mechanism of ta-C:P films can be described by a subimplantation process proposed by Davis and Robertson [27,28]. Here the depositing species for ta-C:P films synthesis are carbon and PH_x plasma. When the energetic grade is lower (-20 V bias), the mixed plasma cannot overcome the restriction of substrate surface and exhibits a surface growth. The moderate energetic grade (-80 V bias) promotes the ability of the plasma to penetrate into the surface either by direct entry or by the displacement of a surface atom into an interstitial site in the subsurface. This network is rearranged by the densification of sp^3-hybridized carbon atoms and the clustering of sp^2 sites induced by phosphorus atoms in local areas. At the subhigh energetic grade (-200 V bias), the particles randomly displace carbon or phosphorus atoms from their equilibrium positions in the subsurface again back onto the surface by releasing thermal energy. At the highest energetic grade (-2000 V bias), the dissipation is more drastic with the effusion of more active phosphorus atoms. The sp^2 sites are further released to form higher-ordering ring structures under the effect of the ‘‘thermal spikes’’. Thereby the deposition process of ta-C:P films indicates a dynamic balance of surface growth and surface damage.

4. Conclusions

The filtered cathodic vacuum arc technique is used to prepare phosphorus incorporated tetrahedral amorphous carbon (ta-C:P) films with the implantation of PH_3 dopant. The effect of substrate bias on the growth process and structural properties of ta-C:P films is discussed via the analyses of XPS, AFM, Raman, intrinsic stress, optical and electrical behaviors. It can be inferred that the amorphous structures of ta-C:P films do not change with phosphorus incorporation. An optimum −80 V bias is observed to benefit the implantation of phosphorus. At the lower bias from −20 to −200 V, phosphorus impurities increase the sp^2 cluster. While at the higher −2000 V bias higher-energetic impinging ions evidently facilitate sp^2 sites to form higher-connected ring structures. The second-order Raman bands of carbon validate the existence of small graphitic crystallites based on a finite-crystal-size effect. Furthermore, phosphorus impurities and high bombardment energy lead to the relief in intrinsic compressive stress, the reduction in optical gap and the increase in the conductivity for ta-C:P films. The deposition process of ta-C:P films is controlled by the subimplantation model.

Acknowledgments

The authors would like to thank the National Natural Science Foundation of China (Grant No. 50602012) for its financial support and Dr. Sun Mingren, Chen Yajie, Wang Jinghe and Zhao Guijie for their assistance provided in doing XPS, Raman, AFM and optical measurements.

References

[1] M. Rusop, X.M. Tian, T. Kinugawa, T. Soga, T. Jimbo, M. Umeno, Appl. Surf. Sci. 252 (2005) 1693.
[2] L.K. Cheah, X. Shi, E. Liu, Appl. Surf. Sci. 143 (1999) 309.
[3] V.S. Veerasamy, G.A.J. Amaratunga, C.A. Davis, A.E. Timbs, W.I. Milne, D.R. McKenzie, J. Phys.: Condens. Matter 5 (1993) Ll69.
[4] K.M. Krishna, M. Umeno, Y. Nukaya, T. Soga, T. Jimbo, Appl. Phys. Lett. 77 (2000) 1472.
[5] G.M. Fuge, P.W. May, K.N. Rosser, S.R.J. Pearce, M.N.R. Ashfold, Diam. Relat. Mater. 13 (2004) 1442.
[6] S.C.H. Kwok, J. Wang, P.K. Chu, Diam. Relat. Mater. 14 (2005) 78.
[7] M. Rusop, T. Soga, T. Jimbo, Sol. Energy Mat. Sol. C 90 (2006) 291.
[8] C.L. Tsai, C.F. Chen, C.L. Lin, J. Appl. Phys. 90 (2001) 4847.
[9] S.R.J. Pearce, J. Filik, P.W. May, R.K. Wild, K.R. Hallam, P.J. Heard, Diam. Relat. Mater. 12 (2003) 979.
[10] J.Q. Zhu, J.C. Han, S.H. Meng, J.H. Wang, W.T. Zheng, Vacuum 72 (2004) 285.
[11] A.S. Argon, V. Gupta, H.S. Landis, J.A. Cronie, Mater. Sci. Eng. A 107 (1989) 41.
[12] C. Oppedisano, A. Tagliaferro, Appl. Phys. Lett. 75 (1999) 3650.
[13] F. Claeyssens, G.M. Fuge, N.L. Allan, P.W. May, M.N.R. Ashfold, Dalton. Trans. 19 (2004) 3085.
[14] E. Kurita, Y. Tomonaga, S. Matsumoto, K. Ohno, H. Matsuura, J. Mol. Struc. Theochem. 639 (2003) 53.
[15] G. Messina, A. Paoletti, S. Santangelo, A. Tagliaferro, A. Tucciarone, J. Appl. Phys. 89 (2001) 1053.
[16] R.B. Wright, R. Varma, D.M. Gruen, J. Nucl. Mater. 63 (1976) 415.
[17] N.M.J. Conway, A.C. Ferrari, A.J. Flewitt, J. Robertson, W.I. Milne, A. Tagliaferro, W. Beyer, Diam. Relat. Mater. 9 (2000) 765.
[18] A.C. Ferrari, J. Robertson, Phys. Rev. B 61 (2000) 14095.
[19] M.M. Golzan, D.R. McKenzie, D.J. Miller, S.J. Collocott, G.A.J. Amaratunga, Diam. Relat. Mater. 4 (1995) 912.
[20] E.G. Gerstner, P.B. Lukins, D.R. McKenzie, D.G. McCulloch, Phys. Rev. B 54 (1996) 14504.
[21] R.J. Nemanich, S.A. Solin, Phys. Rev. B 20 (1979) 392.
[22] Y.J. Lee, J. Nucl. Mater. 325 (2004) 174.
[23] M.C. Polo, J.L. Andujar, A. Hart, J. Robertson, W.I. Mine, Diam. Relat. Mater. 9 (2000) 663.
[24] M. Chhowalla, Y. Yin, G.A.J. Amaratunga, D.R. McKenzie, Th. Frauenheim, Appl. Phys. Lett. 69 (1996) 2344.
[25] A.C. Ferrari, S.E. Rodil, J. Robertson, W.I. Milne, Diam. Relat. Mater. 11 (2002) 994.
[26] J. Robertson, Philo. Mag. B 76 (1997) 335.
[27] C.A. Davis, Thin Solid Films 226 (1993) 30.
[28] J. Robertson, Diam. Relat. Mater. 2 (1993) 984.